

Vasoregulation by the $\beta 1$ subunit of the calcium-activated potassium channel

Robert Brenner¹, Guillermo J. Pérez¹, Adrian D. Bonev², Debrae M. Eckman³, Jon C. Kosek¹, Steven W. Miller¹, Andrew J. Patterson³, Mark T. Nelson¹ & Richard W. Aldrich¹

¹ Department of Molecular and Cellular Physiology and Howard Hughes Medical Institute, Stanford University, Stanford, California 94305, USA

² Department of Pharmacology, College of Medicine, The University of Vermont, Burlington, Vermont 05405, USA

³ Department of Pathology, Palo Alto Veterans Administration Healthcare System, Palo Alto, California 94305 and Stanford University School of Medicine, Stanford, California 94305, USA

⁴ Department of Anesthesiology, Stanford University School of Medicine, Stanford, California 94305, USA

Small arteries exhibit tone, a partially contracted state that is an important determinant of blood pressure. In arterial smooth muscle cells, intracellular calcium paradoxically controls both contraction and relaxation. The mechanisms by which calcium can differentially regulate diverse physiological responses within a single cell remain unresolved. Calcium-dependent relaxation is mediated by local calcium release from the sarcoplasmic reticulum. These 'calcium sparks' activate calcium-dependent potassium (BK) channels comprised of α and $\beta 1$ subunits. Here we show that targeted deletion of the gene for the $\beta 1$ subunit leads to a decrease in the calcium sensitivity of BK channels, a reduction in functional coupling of calcium sparks to BK channel activation, and increases in arterial tone and blood pressure. The $\beta 1$ subunit of the BK channel, by tuning the channel's calcium sensitivity, is a key molecular component in translating calcium signals to the central physiological function of vasoregulation.

Chronic blood pressure elevation resulting from increased arterial tone creates a burden on many organs leading to stroke, heart disease and renal disease¹. An understanding of the molecules involved in regulating arterial tone is crucial to improving our understanding of essential hypertension and perhaps to developing better therapies. Large-conductance calcium-activated potassium channels (BK channels) are pivotal in the regulation of arterial tone, where they facilitate a negative feedback mechanism which opposes vasoconstriction². Intravascular pressure increases arterial tone by a complex process which includes a graded membrane depolarization and elevation of calcium influx through dihydropyridine-sensitive, voltage-dependent calcium channels^{3,4}. Calcium influx causes a global increase in cytoplasmic calcium leading to vasoconstriction. Calcium influx also activates localized calcium release events from ryanodine receptors, termed calcium sparks, which in turn activate nearby calcium-activated potassium (BK) channels, causing a hyperpolarizing current to oppose vasoconstriction⁵. Arterial tone therefore results from the interplay of opposing calcium-dependent processes: constriction, which is driven by global increases in calcium; and relaxation, which is driven by localized calcium concentrations⁶. The important role of BK channels in smooth muscle is demonstrated when the channels are specifically blocked with iberiotoxin⁷, which leads to marked membrane depolarization and vasoconstriction^{8,9} and inhibits the actions of a variety of smooth muscle relaxants¹⁰.

BK channels are broadly expressed, and have functional roles in vascular smooth muscle as well as other tissues including skeletal muscle, neurons, kidney and secretory cells^{11–16}. The functional diversity required for the tissue-specific roles of BK channels may be created in part by association with accessory β -subunits. A family of four BK β -subunits has been identified^{17–20}. Each family member has a different tissue distribution and different effects on BK channel pharmacology and activation gating. The $\beta 1$ -subunit is enriched in smooth muscle and purifies with the BK pore-forming subunit²¹. In expression systems, the $\beta 1$ subunit confers an increased calcium sensitivity, slows gating kinetics and increases

the sensitivity to the agonist dehydrosapogenin (DHS-1)^{22,23}. Using sensitivity to DHS-1 as a probe for BK $\alpha/\beta 1$ subunits, it has been shown that human coronary artery smooth muscle is enriched for $\alpha/\beta 1$ -assembled BK channels, and that these channels are more calcium sensitive than BK channels in other tissues where the $\beta 1$ subunit is not expressed²⁴.

Although the functional role of the BK $\beta 1$ subunit in native tissues is unknown, the assumption is that the $\beta 1$ subunit may increase calcium sensitivity sufficiently for regulation of smooth muscle membrane properties. However, evidence indicates that BK channels are localized very close to calcium release sites, such that they would be exposed to effectively high calcium concentrations (>10 μ M calcium)²⁵ during calcium release. Thus, it is not known whether the increased BK channel calcium sensitivity conferred by the $\beta 1$ subunit contributes to normal smooth muscle function.

Our hypothesis was that the $\beta 1$ subunit has a central molecular role in conferring specificity to the translation of local calcium signals to long-distance electrical events (that is, membrane hyperpolarization) so as to couple calcium to a decrease in vascular tone and blood pressure. We have used gene targeting to eliminate $\beta 1$ subunit expression in mice and evaluate its contribution to vascular smooth muscle function. We examined the roles of the $\beta 1$ subunit in determining the Ca^{2+} sensitivity of BK channels, and the coupling of Ca^{2+} sparks to BK channel activity in smooth muscle cells from cerebral arteries. Furthermore, the $\beta 1$ knockout mice allowed us to evaluate the functional role of the $\beta 1$ subunit in regulating arterial tone and systemic blood pressure in awake, resting animals.

Our results indicate that the calcium sensitivity of the BK channel is uniquely matched by β -subunit association to a given calcium signalling modality to modulate the physiology of arteries.

Generation of $\beta 1$ knockout mice

To create a null allele of the $\beta 1$ locus, the gene-targeting vector was constructed to delete the first coding exon (exon 2) of the gene²⁶. Exon 2 encodes the amino-terminal coding sequence including the

first transmembrane domain of the $\beta 1$ protein. The targeting vector was designed to insert a β -galactosidase reporter in translational frame with the $\beta 1$ subunit translation initiation site (Fig. 1a), and thus report transcription from the $\beta 1$ gene promoter. Transfection of the targeting construct in embryonic stem cells generated three independent clones that specifically targeted the mouse $\beta 1$ gene. Each of the embryonic stem cell clones was implanted into blastocysts and produced germline transmitting mice. Genomic Southern analysis using DNA fragments to hybridize outside the left and right arms of the targeting vector confirmed the recombination (Fig. 1b), seen as a polymorphism that shifts the bands to a predictable, larger size (Fig. 1). To confirm the disruption of the $\beta 1$ gene, an antisense RNA probe encompassing the N-terminal coding region was used as a probe against RNA extracted from $\beta 1$ knockout and control stomach tissue. RNase protection (Fig. 1c)

reveals a protected $\beta 1$ probe hybridizing to control but not knockout mice RNA, confirming the lack of $\beta 1$ expression in the knockout mice.

$\beta 1$ messenger RNA is enriched in smooth muscle

The $\beta 1$ subunit mRNA has been detected in many tissues containing smooth muscle¹⁵. The lacZ gene was targeted to the $\beta 1$ locus to permit the examination of the cell types that normally express the $\beta 1$ subunit. Figure 2 shows lacZ staining in isolated cerebral arteries used in this study as well as other smooth muscle tissues. Within certain tissues, expression is restricted to arterial smooth muscle. Examples are brain and heart (Fig. 2c, g), where $\beta 1$ expression is largely undetected except in the vasculature, such as the cerebral arteries (Fig. 2b), aorta and coronary arteries (not shown). This is consistent with *in situ* hybridizations of $\beta 1$ RNA, where expression

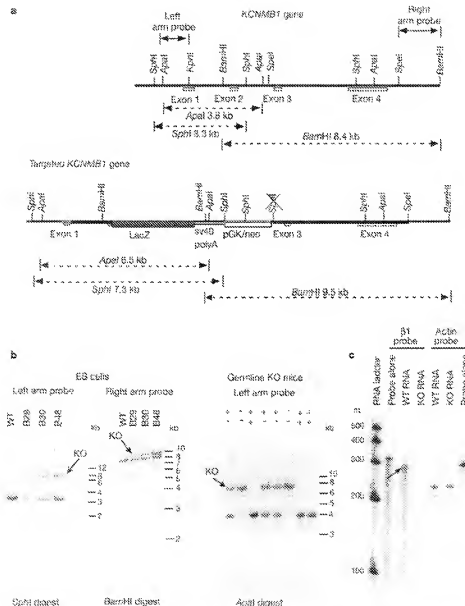


Figure 1 Generation of $\beta 1$ gene knockout mice. **a**, Restriction map of the $\beta 1$ gene locus and the targeting vector. The targeting vector was designed to insert a β -galactosidase reporter in translational frame with the $\beta 1$ subunit translation initiation site (Fig. 1a), and thus report transcription from the $\beta 1$ gene promoter. Transfection of the targeting construct in embryonic stem cells generated three independent clones that specifically targeted the mouse $\beta 1$ gene. Each of the embryonic stem cell clones was implanted into blastocysts and produced germline transmitting mice. Genomic Southern analysis using DNA fragments to hybridize outside the left and right arms of the targeting vector confirmed the recombination (Fig. 1b), seen as a polymorphism that shifts the bands to a predictable, larger size (Fig. 1). To confirm the disruption of the $\beta 1$ gene, an antisense RNA probe encompassing the N-terminal coding region was used as a probe against RNA extracted from $\beta 1$ knockout and control stomach tissue. RNase protection (Fig. 1c)

reveals a protected $\beta 1$ probe hybridizing to control but not knockout mice RNA, confirming the lack of $\beta 1$ expression in the knockout mice.

was enriched in aortic smooth muscle but absent from brain¹⁹. Expression of $\beta 1$ was also observed in other tissues, including smooth muscle of the bladder, trachea, bronchi and the digestive tract (trachea, stomach and colon staining are shown in Fig. 2d–f, respectively).

$\beta 1$ knockout BK channels have reduced Ca^{2+} sensitivity

The fact that the $\beta 1$ subunit is restricted in expression to smooth muscle cells suggested a unique role of the $\beta 1$ subunit in Ca^{2+} signalling in smooth muscle. To confirm that the arterial smooth muscle from the knockout mice lacked a functional $\beta 1$ subunit, the sensitivity of BK channels to calcium and the BK/ $\beta 1$ channel agonist DHS-1 were examined in inside-out patches from freshly isolated cerebral artery myocytes at physiological membrane potentials (-40 mV) for pressurized arteries¹⁵. Figure 3 compares single BK channel recordings of excised patches from knockout and control arterial smooth muscle. BK channels were exposed to cytoplasmic calcium concentrations of 3 and 10 μM , concentrations within the range predicted for calcium-spark-evoked activation of BK channels in arterial smooth muscle⁸. At -40 mV, control BK channels have a significant open probability when activated by 3 μM ($P_o = 0.42 \pm 0.2$) and by 10 μM Ca^{2+} ($P_o = 0.60 \pm 0.2$). In contrast, BK channels from KO cells had an open probability at least 100-fold lower at -40 mV ($P_o = 0.005 \pm 0.002, 0.007 \pm 0.002$ for 3 and 10 μM calcium, respectively). Increasing the membrane voltage to $+40$ mV increases the open probability in both control and KO channels, but the control BK channels still have significantly higher open probability than the BK channels in the knockout cells (control, $P_o = 0.89 \pm 0.03, 0.78 \pm 0.073$; knockout, $P_o = 0.22 \pm 0.07, 0.53 \pm 0.06$ for 3 and 10 μM calcium, respectively).

The agonist DHS-1 significantly increases the open probability of the channels when associated with a $\beta 1$ subunit¹⁹ and provides a pharmacological probe for the presence of BK $\alpha/\beta 1$ -assembled

subunits. Figure 3a shows that application of DHS-1 to the bath causes a significant increase in open probability in control mice ($P_o_{\text{control}} = 0.11 \pm 0.1$ versus $P_o_{\text{DHS-1}} = 0.25 \pm 0.1$; $P < 0.05$, $n = 3$, -40 mV). DHS-1, however, had no effect on the BK channels from $\beta 1$ knockout mice ($P_o_{\text{KO}} = 0.005 \pm 0.001$ versus $P_o_{\text{DHS-1}} = 0.007 \pm 0.001$; $P > 0.4$, $n = 3$, -40 mV). Neither BK channel density, as assayed from the average number of channels detected in patches (Fig. 4b), nor the BK channel unitary conductance (γ), was affected in the knockout ($\gamma_{\text{KO}} = 209 \pm 14$ pS, $\gamma_{\text{control}} = 215 \pm 1.1$ pS, $n = 3$ patches each, from -90 to $+60$ mV in symmetric 145 mM K, $P > 0.4$). The decreased open probability and insensitivity to DHS-1 support the conclusion that BK channels in normal cerebrovascular smooth muscle consist primarily of BK $\alpha/\beta 1$ subunits, whereas the $\beta 1$ knockout mice contain BK channels lacking an associated $\beta 1$ subunit. This is consistent with the LacZ staining demonstrating $\beta 1$ subunit expression in cerebral artery smooth muscle (Fig. 2).

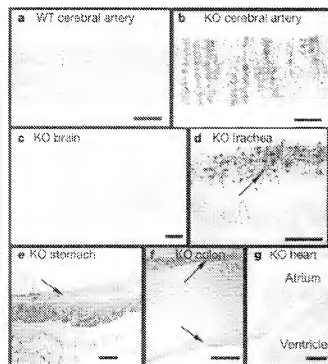


Figure 2 Deletion of the $\beta 1$ gene expression from $\beta 1$ gene-targeted mice. Staining of whole-mount blots (a, b) and frozen sections (c–f) from knockout (KO) and control (WT) mice. Whole staining (arrows) labels regions of $\beta 1$ expression. Scale bars: a, b, d, e, 50 μm ; c, 1 mm; f, 200 μm ; g, 500 μm . Tissues are counterstained with Coomassie Brilliant Blue G250. Scale bars are shown in a, b, d, e, f, g.

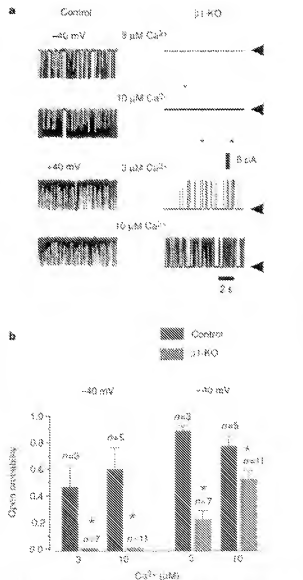


Figure 3 Ca^{2+} and voltage dependence of BK channels in cerebral artery myocytes from control and $\beta 1$ -KO animals. **a**, Single channel recordings in excised patches held at -40 and $+40$ mV, with 3 and 10 μM free Ca^{2+} . Arrows, closed state. Asterisks, brief channel openings in $\beta 1$ -KO patches. **b**, BK channel open probability in control and $\beta 1$ -KO animals in two different voltages (-40 and $+40$ mV) and two Ca^{2+} concentrations (3 and 10 μM). Asterisks denote statistically significant differences from controls.

$\beta 1$ subunit couples calcium sparks to BK channel activation

The open probability of BK channels is low at physiological membrane potentials (-40 mV) and average arterial smooth muscle calcium of pressurized cerebral arteries¹. A calcium spark can elevate the Po of nearby BK channels 10^3 to 10^4 -fold to produce a significant transient membrane potential hyperpolarization (20 mV)^{2,3}. To explore the role of the $\beta 1$ subunit in the communication of calcium sparks to BK channels, we measured calcium sparks and whole-cell potassium currents simultaneously in isolated cerebral artery myocytes⁴. Figure 5a illustrates the life cycle of a spark from a $\beta 1$ knockout mouse, peaking in around 20 ms and then decaying over 200 ms, very similar to control myocytes⁴. Figure 5b shows a representative simultaneous recording of whole-cell current (in blue) and sparks (in red and green). Transient BK current amplitude increases with Ca^{2+} spark amplitude in both control and knockout cells (Fig. 5c). However, the mean transient BK current amplitude was around one-sixth of control amplitude for a given Ca^{2+} spark amplitude. Furthermore, there was a striking difference in the ability of Ca^{2+} sparks to activate transient BK currents. In the control, essentially every Ca^{2+} spark evoked a transient BK current at -40 mV. In contrast, in the knockout 35% of the sparks failed to evoke a detectable BK current (Fig. 5d). BK channel density, Ca^{2+} spark amplitude (control = 1.65 ± 0.03 ($n = 94$ from 6 cells), knockout = 1.77 ± 0.05 ($n = 71$ from 7 cells)), and spark frequency (control = 1.41 ± 0.2 Hz (6 cells), and knockout = 1.35 ± 0.3 Hz (7 cells)) were unaltered in the knockout. These results indicate that the overall BK channel activity during Ca^{2+} sparks is reduced at least 12-fold in the knockout, consistent with the diminished Ca^{2+} sensitivity of BK channels (Figs 3 and 4).

Lack of $\beta 1$ elevates arterial tone and blood pressure

BK channels lacking the $\beta 1$ subunit are present and functional in arteries from knockout mice, albeit less sensitive to activating calcium. To understand the physiological consequences of the reduced coupling between calcium sparks and BK channel activation

in the $\beta 1$ knockouts, we evaluated the effect of pressure on arterial diameter. Elevation of intravascular pressure constricts small arteries, including cerebral arteries⁵⁻⁷. Cerebral arteries that lack the $\beta 1$ subunit are significantly more constricted at a given pressure than are control arteries (Fig. 6a-c). These results indicate that the lack of the $\beta 1$ subunit leads to an elevation in arterial tone.

The contribution of the $\beta 1$ subunit to the regulation of arterial tone can be evaluated by examining the effects of the BK inhibitor Iberiotoxin (IBTX) on arterial diameter. IBTX caused a 74% increase in arterial tone in the control (Fig. 6d, f). In contrast, IBTX did not affect knockout cerebral arteries (Fig. 6e, f). These results indicate that BK channels lacking the $\beta 1$ subunit are unable to contribute to the regulation of arterial tone.

Unless systemic physiological control mechanisms can compensate for the increased arterial tone, arterial blood pressure should be elevated in mice lacking the BK $\beta 1$ subunit. The mean arterial blood pressure of the knockout mice was indeed elevated and comparable to transgenic mice with compromised endothelial function⁸. The knockout lines were bred from a mixture of 129svj mice, used to derive the embryonic stem cells, and C57BL mice, used as the initial breeder mates. We chose to compare the mean arterial pressure of our knockout mice to the mean arterial pressure of 129svj control mice to generate the most stringent test for evidence of elevated blood pressure, as the 129svj mice have a higher mean arterial blood pressure than any other strain⁹. The knockout mice exhibited an increase in mean blood pressure, even over the pure 129svj mice (Fig. 7a). These data indicate that the increased arterial tone leads to an elevation in blood pressure.

In humans, long-standing essential hypertension induces significant left ventricular hypertrophy and leads to heart enlargement¹⁰.

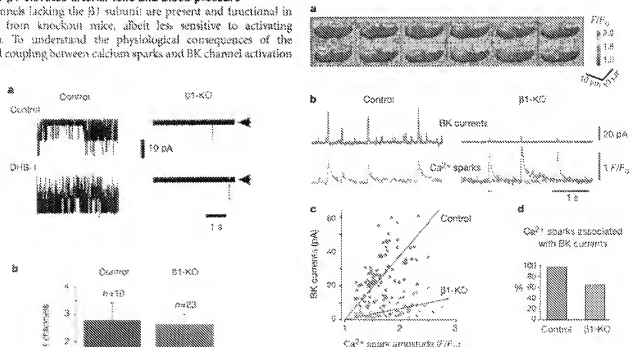


Figure 4 Ca^{2+} sensitivity and density of BK channels in cerebral arteries myocytes from control and $\beta 1$ -KO animals. **a**, Single channel recordings at -40 mV and 10 pA Ca^{2+} before and after the addition of 100 nM [199.1]. **b**, Average increase of channels per patch method from control and $\beta 1$ -KO myocytes. Ca^{2+} and Ca^{2+} patches, respectively. No significant difference was found between control and $\beta 1$ -KO patches. Membrane resistances were 4.1 ± 1 M Ω .

Figure 5 Decreased coupling of calcium sparks to BK channels in $\beta 1$ -KO myocytes. **a**, Correlative pseudocolored three-dimensional images of a $\beta 1$ -KO cell obtained every 233 ms. **b**, Simultaneous BK current (blue) and Ca^{2+} spark measurements (functional fluorescence, F/F_0) from a control cell with one spark site and a $\beta 1$ -KO cell with two spark sites (red and green) (-40 mV). Red bar indicates the segment of the red trace illustrated in **c**. **c**, Relationships between BK current and Ca^{2+} spark amplitudes in control (blue, $n = 94$ sparks, 6 cells) and $\beta 1$ -KO cells (red, 71 sparks, 7 cells). Lines represent linear regression fit (slope_{control} = 34.8 ± 1.6 versus slope $\beta 1$ -KO = 6.1 ± 0.3 , $P < 0.001$). **d**, Percentage of Ca^{2+} sparks causing transient BK currents in control (blue) and $\beta 1$ -KO (red) cells.

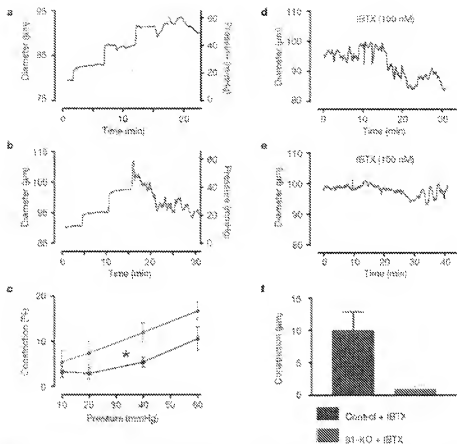


Figure 6 $\beta 1$ KO L-type arteries are more constricted to pressure. **a**, Control; blue. **b**, $\beta 1$ -KO; red. **c**, Summary. $P < 0.05$. They are also insensitive to the BK channel

blocker iberiotoxin. **d**, control; blue; **e**, $\beta 1$ -KO; red. **f**, summary. Grey lines indicate pressure levels in **a** and **b**.

To measure heart enlargement, we normalized the heart weight to animal body weight. Knockout mice had larger heart-to-body weight ratios than 129svj mice (Fig. 7b). Furthermore, at the electron microscopy level, there were no obvious differences in ultrastructure of the cardiomyocytes between the 129svj control hearts and the $\beta 1$ knockout hearts (Fig. 7c). Myofibrillar organization, mitochondrial prevalence and structure, and glycogen content appeared similar in control and knockout mice. There was no evidence of necrosis or fibrosis. As heart muscle ultrastructure appeared normal, these findings are consistent with heart enlargement caused by uncomplicated essential hypertension.

Discussion

The BK channel is the only member of the voltage-dependent potassium channel family that is activated by both voltage and calcium. This makes it particularly suited to integrate calcium and voltage signals to modulate membrane excitability in a variety of cell types. But the tissues that express BK channels have diverse functions with considerable differences in excitability and Ca^{2+} signaling. Our results support the concept that the $\beta 1$ subunit is required specifically to tune BK channel properties to the needs of an arterial smooth muscle cell. The increased sensitivity to calcium conferred by the $\beta 1$ subunit is required for the BK channel to translate calcium sparks to membrane potential hyperpolarization. The decreased coupling of Ca^{2+} to channel activity extrapolated well to the functional defects observed in the intact artery and whole animal. Moreover, and organ pathology observed in chronic hypertension, such as myocardial hypertrophy, was also observed in the BK $\beta 1$ knockout mice. The BK $\beta 1$ knockout mouse therefore presents a unique model, wherein a clearly defined molecular defect could be used to study the secondary effects of hypertension. Moreover, the

$\beta 1$ subunit gene should provide a candidate genetic locus for human hypertension.

Not only was BK channel activity reduced when the $\beta 1$ subunit was absent, as detected by the reduced size of transient BK currents, but many calcium sparks failed to cause detectable currents. The most direct explanation is that the calcium sensitivity of the BK channel lacking $\beta 1$ is reduced sufficiently so that the channel open probability during a spark is too low to cause a detectable current (one single BK channel amplitude at ~ 10 pA, or 2 pA). The effect is to uncouple BK channel activation from calcium spark signals. Further evidence of uncoupling was the lack of effect of iberiotoxin on arterial tone in $\beta 1$ knockout arteries. It has been estimated that BK channels in the presence of $\beta 1$ subunits appose close enough to calcium release sites to detect 10^{-10} – 10^{-9} M effective calcium concentrations¹⁶. In $10 \mu\text{M}$ calcium, cloned vascular smooth muscle BK channels lacking a $\beta 1$ subunit have a voltage for half activation of around $+30$ mV¹⁶, and have a very low open probability at -40 mV, the membrane potential of smooth muscle in intact pressurized arteries. In contrast, the same channels containing the $\beta 1$ subunit have activation voltages 70 mV more negative¹⁶, at approximately the resting membrane potential for smooth muscle cells (-40 mV). Thus, the reduced apparent calcium sensitivity can explain the difference in spark/BK current coupling between the knockout mice and their controls. However, this does not exclude the possibility that the $\beta 1$ subunit may have other effects on BK channel properties. For example, $\beta 1$ subunits could be required for subcellular localization of BK channels to calcium release sites or modifying BK channel phosphorylation-dependent regulation.

The BK channel regulates arterial diameter and mediates the response to a number of smooth muscle relaxants including nitric

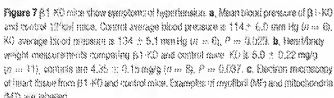


Figure 7 $\beta 1$ -KO mice show symptoms of hypertension. **a**, Mean blood pressure of $\beta 1$ -KO and control $129/SvEv$ mice. Corent average blood pressure is 114 ± 6.0 mm Hg ($n = 6$), KO average blood pressure is 134 ± 5.1 mm Hg ($n = 6$), $P = 0.023$. **b**, Heart/body weight measurements comparing $\beta 1$ -KO and control mice. KO is 0.50 ± 0.22 mg/g ($n = 11$), controls are 0.45 ± 0.15 mg/g ($n = 9$), $P = 0.037$. **c**, Electron microscopy of heart tissue from $\beta 1$ -KO and control mice. Examples of myofibril DMFs and mitochondria (left) are shown.

oxide²⁴⁻²⁶. Our results support the concept that the calcium sensitivity of the BK channel is fine tuned to respond to calcium signals unique to the physiology of a given cell type. In the case of arterial smooth muscle, the $\beta 1$ subunit is essential for the effective coupling of calcium sparks to BK channels, thereby enabling BK channel regulation of arterial smooth muscle tone. In different tissues, other β -subunit family members may serve similar roles. Furthermore, we propose that other agents, such as cyclic AMP- and cGMP-mediated vasodilators, which modulate the calcium sensitivity of the BK channels, can dynamically match calcium signals to BK channel activation to regulate cell function.

3.1 knockout mice

The authors are grateful to the referees for their valuable comments.

[illegible]

DNA and RNA analysis

Genomic Southern analysis was as described¹⁰. To make an antisense β1 RNA, nucleotides 1–290 of the coding portion of the mouse β1 complementary DNA were subcloned into the vector pSP65⁺ and transcribed using the T7 RNA polymerase promoter. Ribosome protection assays were conducted using the Ambion RPP30 kit according to the manufacturer's protocol (Ambion). Hybridization was conducted with 1 µg of poly(A)⁺ purified stomach RNA at 42°C for 1 h or 200 ng total stomach RNA at 60°C for 30 min.

LacZ staining of tissue and electron microscopy

Fluorescein isothiocyanate (FITC) was fixed in 0.2% glutaraldehyde in PBS, washed three times in

PRG and then stained for β -galactosidase activity as described³⁶. The tissues were counterstained with Fast Green F (Dainton Co). Electron microscopy of heart tissue was done as described³⁷.

Tissue preparation

♀ larvae of selected male (12569 or 12569X66) of either sex were killed by exanguination while under deep pentathicidal anaesthesia (dipteromorphin; 150 mg/kg body weight). Carotid arteries were rapidly dissected where the brain was submerged in cold (4°C) oxygenated 19% O₂/5% CO₂ physiological saline solution (PSS) of the following composition (in mmol/l): 118.5 NaCl, 4.7 KCl, 24 NaHCO₃, 7.18 KH₂PO₄, 2.5 CaCl₂, 1.2 MgCl₂, 0.24 NaH₂PO₄, 1.16 glucose.

Diameter measurements

We measured the diameter of middle cerebral artery segments by video edge detection, in oxygenated PSS at 37 °C and pH 7.4, with 1, 2, 4, 8, 16, 32, 64, 128, 256, 512, 1024, 2048, 4096, 8192, 16384, 32768, 65536, 131072, 262144, 524288, 1048576, 2097152, 4194304, 8388608, 16777216, 33554432, 67108864, 134217728, 268435456, 536870912, 1073741824, 2147483648, 4294967296, 8589934592, 17179869184, 34359738368, 68719476736, 137438953472, 274877906944, 549755813888, 1099511627776, 2199023255552, 4398046511104, 8796093022208, 17592186044416, 35184372088832, 70368744177664, 140737488355328, 281474976710656, 562949953421312, 1125899906842624, 2251799813685248, 4503599627370496, 9007199254740992, 18014398509481984, 36028797018963968, 72057594037927936, 144115188075855872, 288230376151711744, 576460752303423488, 1152921504606846976, 2305843009213693952, 4611686018427387904, 9223372036854775808, 18446744073709551616, 36893488147419103232, 73786976294838206464, 147573952589676412928, 295147905179352825856, 590295810358705651712, 1180591620717411303424, 2361183241434822606848, 4722366482869645213696, 9444732965739290427392, 18889465931478580854784, 37778931862957161709568, 75557863725914323419136, 151115727451828646838272, 302231454903657293676544, 604462909807314587353088, 1208925819614629174706176, 2417851639229258349412352, 4835703278458516698824704, 9671406556917033397649408, 19342813113834066795298816, 38685626227668133590597632, 77371252455336267181195264, 154742504910672534362390528, 309485009821345068724781056, 618970019642690137449562112, 1237940039285380274899124224, 2475880078570760549798248448, 4951760157141521099596496896, 9903520314283042199192993792, 19807040628566084398385987584, 39614081257132168796771975168, 79228162514264337593543950336, 158456325028528675187087900672, 316912650057057350374175801344, 633825300114114700748351602688, 1267650600228229401496703205376, 2535301200456458802993406410752, 5070602400912917605986812821504, 10141204801825835211973625643008, 20282409603651670423947251286016, 40564819207303340847894502572032, 81129638414606681695789005144064, 162259276829213363391578010288128, 324518553658426726783156020576256, 649037107316853453566312041152512, 1298074214633706907132624082305024, 2596148429267413814265248164610048, 5192296858534827628530496329220096, 10384593717069655257060992658440192, 20769187434139310514121985316880384, 41538374868278621028243970633760768, 83076749736557242056487941267521536, 166153499473114484112975882535043072, 332306998946228968225951765070086144, 664613997892457936451903530140172288, 1329227995784915872903807060280344576, 2658455991569831745807614120560689152, 5316911983139663491615228241121378304, 10633823966279326983230456482242756608, 21267647932558653966460912964485513216, 42535295865117307932921825928971026432, 85070591730234615865843651857942052864, 170141183460469231731687303715884105728, 340282366920938463463374607431768211456, 680564733841876926926749214863536422912, 1361129467683753853853498429727072845824, 2722258935367507707706996859454145691648, 5444517870735015415413993718908291383296, 10889035741470030830827987437816582766592, 21778071482940061661655974875633165533184, 43556142965880123323311949751266331066368, 87112285931760246646623899502532662132736, 174224571863520493293247799005065324265472, 348449143727040986586495598010130648530944, 696898287454081973172991196020261297061888, 1393796574908163946345982392040522594123776, 2787593149816327892691964784081045188247552, 5575186299632655785383929568162090376495104, 11150372599265311570767859136324180752990208, 22300745198530623141535718272648361505980416, 44601490397061246283071436545296723011960832, 89202980794122492566142873090593446023921664, 178405961588244985132285746181186892047843328, 356811923176489970264571492362373784095686656, 713623846352979940529142984724747568191373312, 1427247692705959881058285969449495136382746624, 2854495385411919762116571938898990272765493248, 5708990770823839524233143877797980545530986496, 11417981541647679048466287755595961091061972992, 22835963083295358096932575511191922182123945984, 45671926166590716193865151022383844364247891968, 9134385233318143238773030204476

Electrical and optical measurements

Single smooth muscle cells were isolated from cerebral arteries by digestion in 5 mg/ml papain and 1 mg ml⁻¹ dithioerythritol for 10 min, and then transferred for 2 sec and digested in 1 mg ml⁻¹ collagenase type I and type IV in a 20%–80% mixture for 7 min at 37°C. Membrane current and calcium spikes were measured simultaneously in myocytes loaded with the Ca²⁺ indicator fura-2, using perforated patch, whole-cell configuration and a laser (two-dimensional) scanning confocal microscope.¹⁶ The perfusing solution (in mM): 134 NaCl, 9 KCl, 3 MgCl₂, 2 CaCl₂, 10 glucose, 10 HEPES pH 7.4, with 3 µM thapsigargin to minimize contraction. The pipette solution contained (in mM): 110 K-aspartate, 30 KCl, 10 NaCl, 1 MgCl₂, 10 HEPES pH 7.2 and 250 ng/ml amphotericin B. Single BK channels were recorded in inside-out patches, exposed to cellulose acetate "buffered" solutions (in mM): 140 KCl, 10 HEPES pH 7.3, 3 Mg²⁺, 10 CsF, 10 EGTA, 10 DTPA, 10 Tris-Glycine, 10 Tris-Hydroxybutyrate, 10 Tris-Maleate, 10 Tris-maleate, 10 mM, 140 KCl, 10 HEPES pH 7.2, 3 Mg²⁺, 5 HEDTA and 10 µM Ca²⁺. Single channel currents were recorded over 10–10-min at steady potential of -40 and +10 mV at room temperature. Currents were induced at 1 kHz and inhibited at 4 kHz.

Blood pressure analysis and heart/body weight ratios

Mean arterial blood pressures were obtained using arterial catheters surgically inserted into the left carotid artery as described¹⁷. Following surgery, animals were allowed to recover for 7 d; at mean arterial blood pressure was measured every 5 s for 30 min, average mean arterial blood pressure values obtained during the sampling period were calculated for each animal. All measurements were performed while the animal resting quietly. To obtain heart weights, isolated beating hearts were dissected free and allowed to bleed the blood volume in saline solution. Hearts were transferred to 1 M PEG-800 and frozen for 15–30 s, sectioned in saline, blotted free of excess solution and weighed. For blood pressure measurements the known animal weight had a mean age of 19.7 ± 2.2 weeks, and control animals were 20.7 ± 3.5 weeks. For heart/body weight, the rats were divided into two groups: low birth weight ($n = 6$) and high birth weight ($n = 6$). The low birth weight group had a body weight at weaning (15 d) of 158 ± 9 g whereas of the high birth weight group (known), 158 ± 9 g. Both groups. Our data and several others do not correlate between littering size and newborn weights or offspring sizes^{23–25}.

Data analysis

Image and BK current analysis was performed using a custom written analysis program using Interactive Data Language software (Research Systems Inc., Burlington, MA). I_{CaT} was determined by averaging 10 images with no activity. Practical thresholding (I_{CaT}) versus time traces were obtained by averaging I_{CaT} from a box region of $2 \times 2 \times 2 \mu\text{m}$ centred in the active area of interest (Ca^{2+} apical shell). Transient Ca^{2+} currents (as Ca^{2+} sparks with amplitudes larger than a single Ca^{2+} channel opening (2 pA , at -100 mV) were considered not further analysis. Number of channels (n) at each probability (P_{Ca}) of single channel current was calculated from all points (frequency \times divided by the number of channel events in the patch to obtain P_{Ca} values).

Statistical analysis

Results are expressed as means \pm s.e.m. where applicable. Comparisons between control and knockout data were done with the unpaired two-tailed student's *t*-test.

Received 15 October 2004; accepted 15 November 2004

2. Jiral JL, Zlotnik-Morgan P, & Narbonne JF. Interleukin-17: a novel effector molecule and inducer of both mucosal and systemic antiviral humoral and cellular responses. *J Virol* 2008; 82: 435–452 [PubMed].
3. Rogovin H, Pines A, Yalovsky J, & Shoham M. IL-17 is a novel effector molecule. *Ann NY Acad Sci* 2008; 1143: 1–10 [PubMed].
4. Lefebvre M, et al. Pathogenesis and characteristics of a unique, persistent periodontitis: the high-mucosin-associated periodontitis in transgenic mice presents the common features of human IL-17. *Cell Tissue Res* 2006; 304: 147–156 [PubMed].
5. Lefebvre M, et al. Interleukin-17 is a novel effector molecule in periodontitis. *J Biol Chem* 2006; 281: 16246–16250 [PubMed].
6. Lefebvre M, Bouchard S, & Narbonne JF. Interleukin-17 is a novel effector molecule in periodontitis. *J Biol Chem* 2006; 281: 16246–16250 [PubMed].
7. Streeter M, & Narbonne JF. Regulation of anterior horn by activation of cytokine-dependent neurons. *J Neurosci* 2008; 28: 1230–1239 [PubMed].

- [illegible]